

# Wind turbine control based on a permanent magnet synchronous generator connected to a rectifier NPC of three levels

**GASMI Nadia**

PEESE (Processes, Energetics, Environments  
& Electrical Systems) research laboratory  
LR18ES34  
National Engineering school of Gabes, Tunisia  
Email: [gasminadia809@hotmail.com](mailto:gasminadia809@hotmail.com)

**BEN HAMED Mouna**

PEESE (Processes, Energetics, Environments  
& Electrical Systems) research laboratory  
LR18ES34  
National Engineering school of Gabes, Tunisia  
Email: [benhamed2209@yahoo.fr](mailto:benhamed2209@yahoo.fr)

**Abstract—** This research work develops dynamic model of a gearless small-scale wind power generation system based on a direct driven single sided outer of a Permanent Magnet Synchronous Generator (PMSG). Dynamic modeling of the PMSG based wind turbine requires machine parameters. A three-level rectifier is used as the power converters of wind turbine systems because of their advantages such as low-current total harmonic distortion, high efficiency, and low collector-emitter voltage. permanent magnet synchronous generators (PMSG) have been chosen as the generator in wind turbine systems owing to their advantages of size and efficiency. In wind turbine systems consisting of the three-level rectifier and the PMSG, A maximum power point tracking (MPPT)-based FOC control approach is used to obtain maximum power from the variable wind speed. The simulation results show the proper performance of the developed dynamic model of the PMSG, of the rectifier NPC of three level, control approach and power generation system.

**Keywords—** wind speed ; MPPT;simulation MATLAB software; PMSG;FOC;SVPWM;rectifier NPC of three level.

## I. INTRODUCTION

The use of the renewable energy source as wind energy in the isolated sectors and the rural zones is a better solution to produce the needed electric energy for such applications as the pumping systems [4,11]. During the last decades, the renewable energy system has witnessed a real evolution worldwide. The generation of electric power from renewable energy sources such as wind is very efficient in reducing environment pollution in proving an alternative for the insufficiency of the traditional sources. The wind energy source is rapidly growing and has the highest percentage in terms of installation compared to other energy sources. The wind energy conversion system studied in this article is composed of a wind turbine, a permanent magnet synchronous generator connected to a power grid through rectifier NPC of three level consisting of a

AC/DC interface followed by a second DC/AC interface, and a Inverter NPC of three level that are connected to rectifier NPC of three level as shown in Fig. 1.

It is composed of a three-phase PMSG connected to a rectifier, Field-oriented control (FOC) applied to the generator side converter. The rectifier is controlled by Space Vector Pulse Width Modulation (SVPWM) and ensures the injection of the produced power to the AC grid. The inverter is controlled by Space Pulse Width Modulation (SPWM).

## II. MODELING OF TURBINE

The wind turbine is used for the conversion of wind kinetic energy to mechanical work. On the basis of relationships for the calculation, it is possible to express the value  $P_m$  of the aerodynamic wind turbine power [3].

$$P_m = 0.5C_p(\lambda, \beta)\rho\pi R^2 V_w^3 \quad (1)$$

Where  $V_w$  is the wind speed,  $\rho$  is the air density (typical value is 1.225 kg/m<sup>3</sup>),  $A = \pi \cdot R^2$  is the blades swept of the turbine,  $R$  is the radius of the wind turbine,  $C_p$  is the wind turbine power coefficient,  $\lambda$  is the tip-speed ratio,  $\omega_w$  is the angular rotor Speed for the wind turbine and  $\beta$  is the pitch angle.

$$\left(\frac{116}{\lambda_i} - 0.4\beta - 5\right) \exp^{-\frac{21}{\lambda_i}} + 0.0068 \quad (2)$$

where  $\lambda_i$  is given by

$$\frac{1}{\lambda_i} = \frac{1}{\lambda + 0.08\beta} - \frac{0.035}{\beta^3 + 1} \quad (3)$$

The relationship between the wind speed and the rotor speed is defined as tip speed ration  $\lambda$ : [3]

$$\lambda = \frac{\omega_w R}{V_w} \quad (4)$$

Where  $R$  and  $\omega_w$  are the blade length (in m) and the wind turbine rotor speed (in rad/sec), respectively. The wind turbine mechanical torque output  $T_m$  given as:

$$C_m = \frac{1}{2}\rho\pi R^3 \frac{V_w^2}{\lambda} C_p \quad (5)$$

The aerodynamic turbine power curves family with varying the turbine rotor speed for different value of wind speed.

### III. MECHANIC MODEL

The fundamental dynamic equation is described with the following equation [2]:

$$J \frac{d\Omega}{dt} = T_t - T_{em} - f\omega \quad (6)$$

Where  $T_{em}$  is the electromagnetic torque,  $f$  is the turbine rotor friction. Then, the wind turbine generator drive that represents the mechanical bloc can be given by:

$$T_t - T_{em} = J \frac{d\Omega}{dt} + f\omega \quad (7)$$

### IV. MODELING OF PMSG

To simplify the response study of the PMSG, it is convenient to transform the equations from the stationary stator frame into the d-q axis using Park transformations. The mathematical model of a PMSG is usually defined in the rotating reference frame d-q as follow [6]

$$\begin{cases} \frac{di_d}{dt} = -\frac{R_s}{L_d} i_d + \frac{1}{L_d} V_d + \frac{L_d}{L_q} \rho \omega_r i_q \\ \frac{di_q}{dt} = -\frac{R_s}{L_q} i_q + \frac{1}{L_q} V_q + \frac{L_d}{L_q} \rho \omega_r i_d - \frac{\lambda \rho \omega_r}{L_q} \end{cases} \quad (8)$$

The electromagnetic torque equation is given by [6]

$$T_e = 1.5p[\lambda i_q + (L_d - L_q)i_d i_q] \quad (9)$$

There,  $i_{sd}$ ,  $i_{sq}$ ,  $u_{sd}$ , and  $u_{sq}$  are the d-axis and q-axis currents and voltages respective stator resistance;  $\omega_s$  is the basic electrical angular frequency of the generator;  $L_{sd}$  and  $L_{sq}$  are the inductance of generator;  $\psi_p$  is permanent flux;  $R_{sa}$  is the resistance of stator; and  $P$  is the number of poles.

Figure 2 shows the dq-coordinates frame of the PMSG with  $\theta$  being the angle between d-axis and the main stator axis.

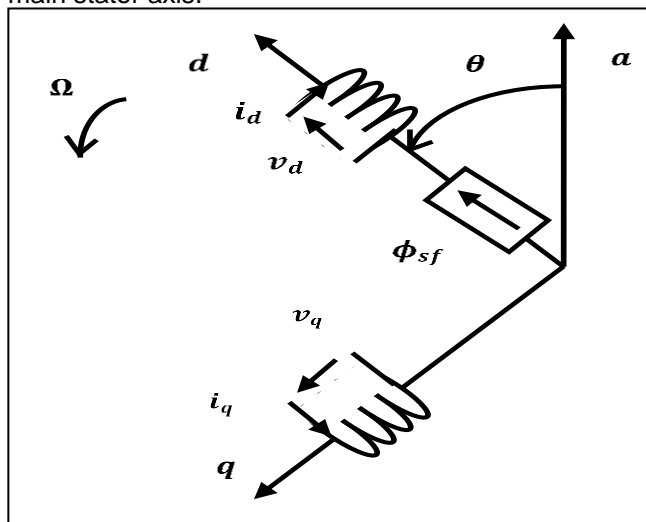
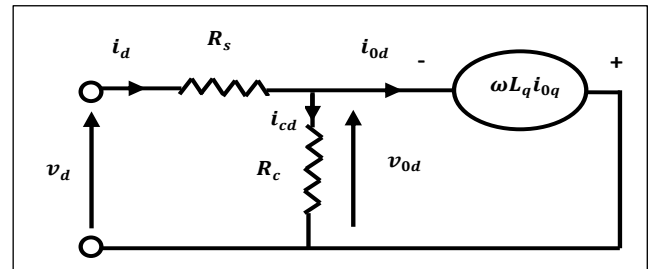


Fig. 2. The dq-coordinate frame of the PMSG[7].

Figure 3 shows the equivalent circuit of the PMSG in de d-q synchronous rotating reference frame.

a) d-axis equivalent circuit[5].



b) q-axis equivalent circuit[5].

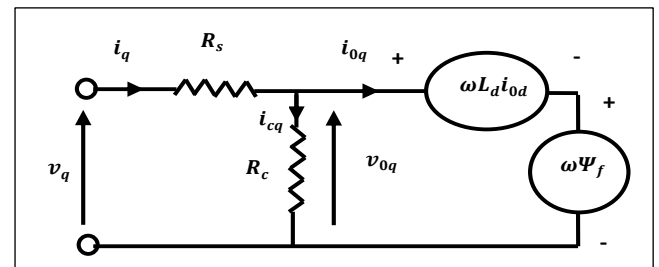


Fig. 3. The equivalent circuit of the PMSG in de d-q.

### V. THE PRINCIPLE AND MODELING OF THREE LEVEL SPWM RECTIFIER

In the neutral point rectifier illustrated in Fig. 4, the converter is built around twelve switching cells (based on IGBT) and six clamping diodes; each phase can produce three distinct levels by connecting the output to the positive ( $V_{dc}/2$ ), negative ( $-V_{dc}/2$ ) or zero (0) potential. In a system three, there are  $3^3 = 27$  output voltage vectors linked to 19 possible voltage vectors at the output of the converter (see Figure 5).

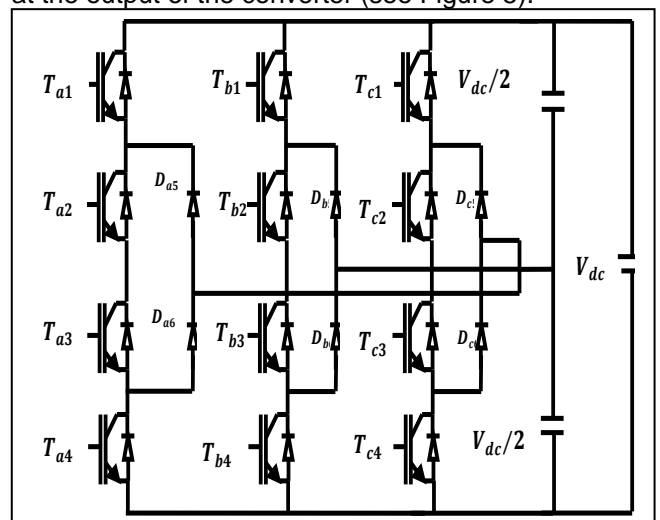


Fig. 4. Topology of NPC three-level PWM rectifier [4].

Switching functions are introduced to describe the states of the NPC three-level PWM rectifier. The expressions below are the switching functions of three legs:

$$S_x = \begin{cases} 2, T_{X1}, T_{X2}: on, T_{X3}, T_{X4}: off \\ 1, T_{X2}, T_{X3}: on, T_{X1}, T_{X4}: off \\ 0, T_{X3}, T_{X4}: on, T_{X1}, T_{X2}: off \end{cases} \quad (10)$$

According to the definition of the switching functions, the equations of the converter can be developed in the three-phase stationary coordinate system abc.

In addition to the line currents, the dynamics of the capacitors is taken into account and is selected as the state variable. However, the phase voltage of the gate and the load current are considered disturbances[8].

$$\begin{cases} u_{sa} = L_s \frac{di_{sa}}{dt} + R_s i_{sa} + S_{a1} V_{dc1} - S_{a2} V_{dc2} + u_{on} \\ u_{sb} = L_s \frac{di_{sb}}{dt} + R_s i_{sb} + S_{b1} V_{dc1} - S_{b2} V_{dc2} + u_{on} \\ u_{sc} = L_s \frac{di_{sc}}{dt} + R_s i_{sc} + S_{c1} V_{dc1} - S_{c2} V_{dc2} + u_{on} \end{cases} \quad (11)$$

$$\begin{cases} c_d \frac{du_{dc1}}{dt} = S_{a1} i_{sa} + S_{b1} i_{sb} + S_{c1} i_{sc} - i_L \\ c_d \frac{du_{dc2}}{dt} = -S_{a2} i_{sa} - S_{b2} i_{sb} - S_{c2} i_{sc} - i_L \end{cases} \quad (12)$$

Considering that the Electrical Network is three-phase balanced one can write

$$\begin{cases} i_{sa} + i_{sb} + i_{sc} = 0 \\ u_{sa} + u_{sb} + u_{sc} = 0 \end{cases} \quad (13)$$

The voltage  $U_{on}$  is given by the following expression [8]:

$$u_{on} = -\frac{1}{3}(S_{a1} + S_{b1} + S_{c1})u_{dc1} + \frac{1}{3}(S_{a2} + S_{b2} + S_{c2})u_{dc2} \quad (14)$$

## VI. CONTROL STRATEGY OF THE VS-WECS

### A. Maximum Power Point Tracking (MPPT) and Pitch Control

The objective of MPPT controller is to generate the reference velocity command which will enable the VS-WECS to extract maximum power at different wind speeds. For this reason, when the wind speed changes, the velocity of WTG is controlled to follow the maximum power point trajectory and, the optimum rotational speed of the PMSG can be simply estimated as follows [5]:

$$\omega_{m-opt} = \frac{V \lambda_{opt}}{R} \quad (15)$$

The maximum extracted power of the WTG is given as:

$$P_{Turbine-max} = \frac{1}{2} \rho A C_{Pmax} \left( \frac{R \omega_{m-opt}}{\lambda_{opt}} \right)^3 \quad (16)$$

As a result, the MPPT controller computes the optimum velocity of WTG:  $\omega_{m-opt}$  and by regulating the generator speed in different wind velocities, the maximum power  $P_{Turbine-max}$  is extracted. Besides, if the wind speed reached the nominal value of WT, the system of Pitch Angle controller enters in operation

### B. Control strategy of PMSG

Vector control strategy is used to have more preferment results, to control the wind turbine. As given in Equation (8) we have a problem of coupling between d- and q-axis, represented by the terms  $p\omega i_q$  and  $p\omega i_d$ . Vector control concept is recommended, in order to overcome this problem of coupling

#### 1) Vector control strategy :

Vector control strategy is based on the field orientation,  $i_d = 0$ . Then according to (9), since  $\phi_m$  is constant, the electromagnetic torque is directly proportional to  $i_q$  [7]. Two inputs  $V_d$  and  $V_q$  are defined to compensate the cross-coupling terms,

$$v_d = p\omega L_q i_q + u_d \quad (17)$$

$$v_q = -p\omega L_q i_d - e_q + u_q \quad (18)$$

$$e_q = \omega \phi_m \quad (19)$$

$$v_d = L_d \frac{di_d}{dt} + R_a i_d \quad (20)$$

$$v_q = L_q \frac{di_q}{dt} + R_a i_q \quad (21)$$

#### 2) Current regulators :

According to (20) and (21), two separate first-order models in the d-q axis. Thus,

$$\frac{i_d}{v_d} = \frac{1}{(sL_d + R_a)} \quad (22)$$

$$\frac{i_q}{v_q} = \frac{1}{(sL_q + R_a)} \quad (23)$$

Therefore, we obtain two similar PI regulators which used in two independent current loops that one of them controls the q-axis component and the second controls d-component as described.

#### 3) Speed regulators

Using the mechanical equation of wind turbine (7) the transfer function of the wind speed is written by:

$$\omega = \frac{(T_t - T_{em})}{J s + f} \quad (23)$$

Therefore, based on the last model the wind speed regulator is designed by a PI controller. In fact, the speed controller takes as input the error between the reference speed  $\omega_{ref}$  and the actual rotational speed. Where  $\omega_{ref}$  is obtained by  $\lambda$  expression as shown in (4), it can be represented by:

$$\omega_{ref} = \lambda \frac{v_w}{R} \quad (24)$$

Then, the speed controller output presents  $i_{qref}$  that is subtracted by the actual  $i_q$  and the result is the input of the current regulator of the quadrature current component. The direct component has as input the results of the subtraction between the reference direct current  $i_{dref}$  that it is null in our strategy and the



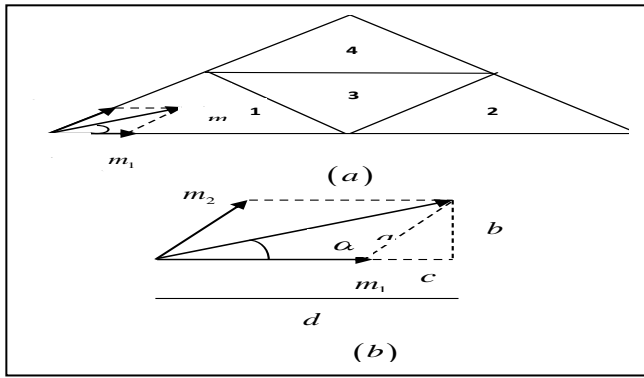


Fig. 6. Space vector diagram for  $m_1$  and  $m_2$  in Sector 'a'[9].

From Figure 6 (b)  $m_1$  and  $m_2$  in sector 'a' can be calculated as

$$m_1 = d - c$$

	Région I	Région II
$T_a$	$2k \sin\left(\frac{\pi}{3} - \theta\right)$	$T_s - 2k \sin \theta$
$T_b$	$T_s - 2k \sin\left(\frac{\pi}{3} + \theta\right)$	$2k \sin\left(\frac{\pi}{3} + \theta\right) - T_s$
$T_c$	$2k \sin \theta$	$T_s - 2k \sin\left(\frac{\pi}{3} - \theta\right)$
	Région III	Région IV
$T_a$	$2k \sin \theta - T_s$	$2T_s - 2k \sin\left(\frac{\pi}{3} + \theta\right)$
$T_b$	$2k \sin\left(\frac{\pi}{3} - \theta\right)$	$2T_s - 2k \sin\left(\frac{\pi}{3} + \theta\right)$
$T_c$	$2T_s - 2k \sin\left(\frac{\pi}{3} + \theta\right)$	$2k \sin\left(\frac{\pi}{3} + \theta\right) - T_s$

$$m_1 = m_n \cos \alpha - \left(\frac{2}{\sqrt{3}} m_n \sin \alpha\right) \cos\left(\frac{\pi}{3}\right) \quad (30)$$

$$m_1 = m_n \left(\cos \alpha - \frac{\sin \alpha}{\sqrt{3}}\right)$$

$$m_1 = m_n \frac{2}{\sqrt{3}} \sin\left(\frac{\pi}{3} - \alpha\right) \quad (31)$$

$$m_2 = a = \frac{b}{\sin\left(\frac{\pi}{3}\right)} = \frac{2}{\sqrt{3}} b = \frac{2}{\sqrt{3}} m_n \sin \alpha \quad (32)$$

$$m_n = \frac{V_{ref}}{\frac{2U_{dc}}{3}} \quad (33)$$

And by,

If the value of  $m_1$ ,  $m_2$  and  $(m_1 + m_2) < 0.5$ , then

$V^*$  lies in **Reg 1**,

If the value of  $m_1 > 0.5$ , then  $V^*$  lies in **Reg 2**,

If the value of  $m_2 > 0.5$ , then  $V^*$  lies in **Reg 3**,

If the value of  $m_1$  and  $m_2 < 0.5$  and  $(m_1 + m_2) > 0.5$ , then  $V^*$  lies in **Reg 4**.

3) Calculating the respective switching times for  $T_a, T_b, T_c$  [9]:

$T_a, T_b, T_c$  switching times of sector 'A' is given in

TABLE II. .  $T_a, T_b, T_c$  switching times of Sector 'a'

4) Finding the switching states based on above step:

At any time by taking the switching transition of only one switch; the switching transition orders are shown below and they are obtained for every region in Sector 'a' if all switching transition states in every region are used. Therefore, switching states for Sector 'a' given below

**Reg 1:** -1-1-1, 0-1-1, 00-1, 000, 100, 110, 111.

**Reg 2:** 0-1-1, 1-1-1, 10-1, 100.

**Reg 3:** 0-1-1, 11-1, 10-1, 100, 110.

**Reg 4:** 00-1, 10-1, 11-1, 110.

may be used as secondary units (in parentheses

## VII. RESULTS AND DISCUSSION

To validate the theoretical study and the effectiveness of the presented control strategy, a complete structure of WECS composed of a variable speed wind turbine, a PMSG, and an electronic power converter connected to the grid are designed under MATLAB Simulink environment.

To examine the tracking effectiveness of the proposed control, a variable wind speed profile is applied as shown in Fig. 8. The simulation parameters are given in Appendix.

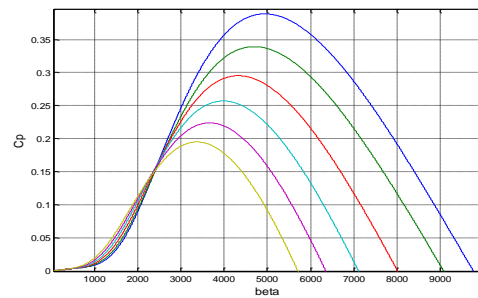


Fig. 7. characteristics for different pitch angle,  $\beta$

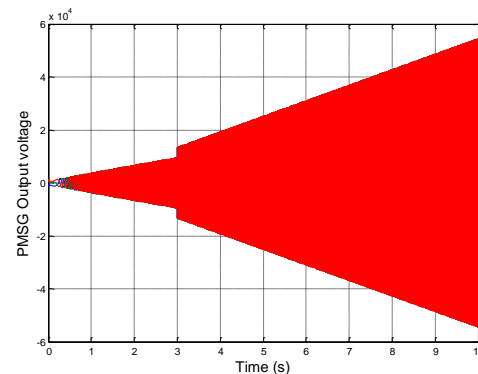


Fig.8.Three Phase Output Voltage of PMSG.

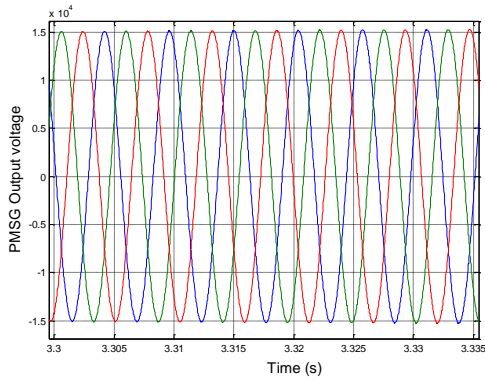


Fig.9.Zoom Three Phase Output Voltage of PMSG

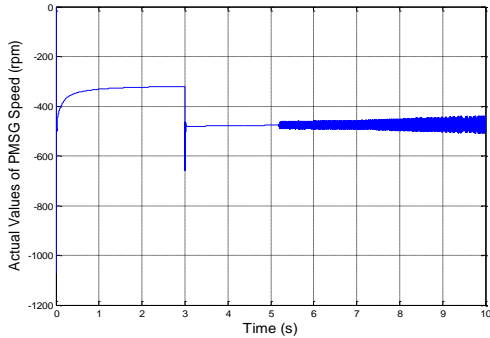


Fig.10.Tracking speed and its reference of PMSG.

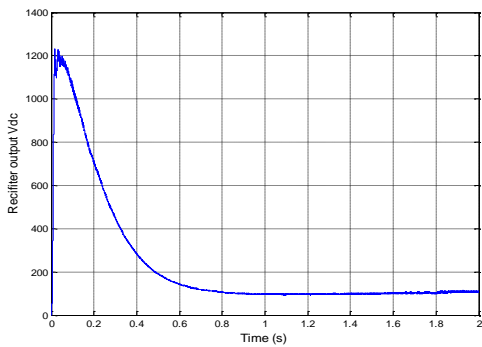


Fig.11. Rectifier Dc output Voltage  $V_{dc}$ .

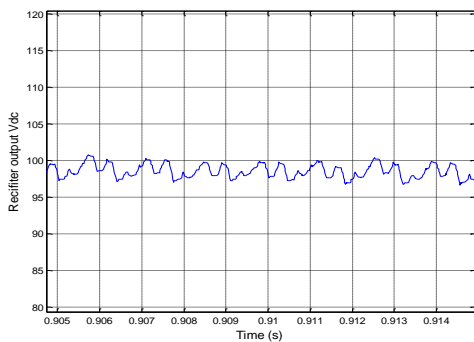


Fig. 12. Zoom Rectifier Dc Output Voltage

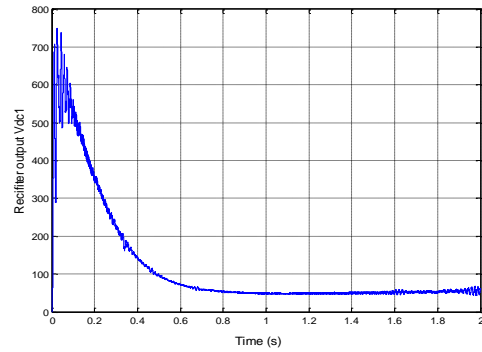


Fig.13. Rectifier Dc output Voltage  $V_{dc1}$ .

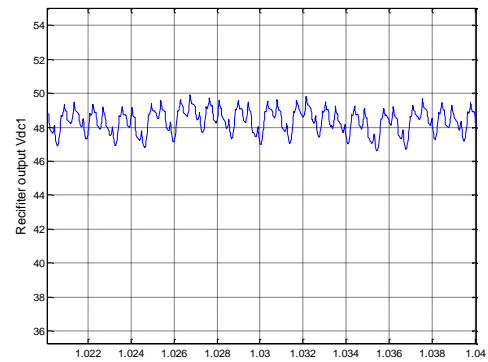


Fig .14. Zoom Rectifier Dc Output Voltage  $V_{dc1}$ .

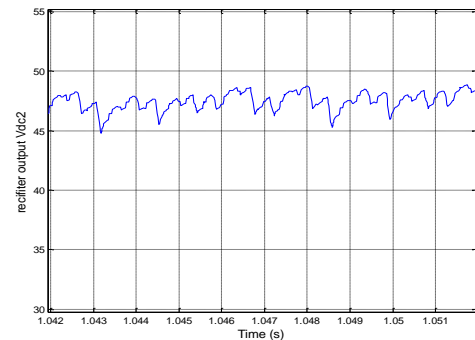


Fig.15.Zoom Rectifier Dc Output Voltage  $V_{dc2}$

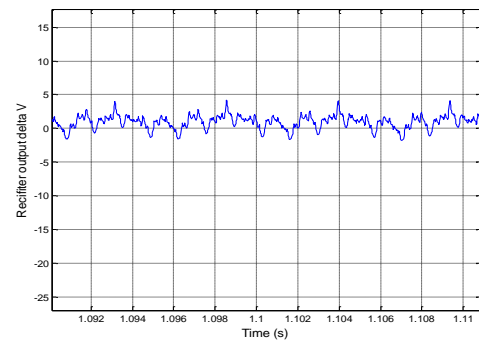


Fig.16.Zoom Rectifier Dc Output Voltage  $\Delta V_{dc}$

## VIII. CONCLUSION

This paper presents the control of the wind energy conversion system using a permanent magnet synchronous generator connected to the rectifier NPC of three level. In order to study the performance, configuration, and control of the system were

presented. SVPWM with FOC has been adapted to minimize the current harmonics. The generator side converter controls the speed of PMSG.

In this paper, A three-phase three-level NPC rectifier was used as PMSG generator side converter to rectify AC output voltage of PMSG wind generator and to build two equal DC voltages. MPPT technique is utilized to produce maximum instantaneous power. Two equal DC voltages were used as input of a three-level NPC inverter to deliver power to grid. The presented simulation results verified higher efficiency and better output characteristics.

Modeling and simulation results of a PMSG based wind turbine system is analyzed and presented in this paper using MATLAB/SIMULINK tool.

#### ACKNOWLEDGMENT

We thank to the Department of Electrical Engineering (PEESE (Processes, Energetics, Environments & Electrical Systems) research laboratory LR18ES34). We would also like to thank, Mouna BEN HAMMED, Lassaad SBITA the who helped us prepare the material in this study and would not forget all those involved directly and indirectly in completing this study

#### APPENDIX

TABLE III. Wind turbine Parameters[10].

Parameters	value
Blade raduis	1.26m
Max. power conv. Coeff.	0.45
Optimal tip speed ratio	7
Cut-in speed	3m/s
Rated wind speed	13m/s
Gear ratio	1

TABLE IV. PMSG machine Parameters[10].

Parameters	value
Rated power	3KW
Rated line voltage	220V
Stator resistance	0.49Ω
Inductance	5.35mH
Torque constant	2.4Nm/A
Back-emf constant	147V/Krpm
Number of poles	6
Rated frequency	60Hz
Generator efficiency	87.3%

TABLE V. NPC rectifier system parameters[11]

Parameters	Value
Line resistance $R_s$	0.3Ω
Line inductance $L_s$	5mH
Switching period $T_s$	0.5e-3s
DC capacitor $C_d$	5mF
Resistor load $R_L$	100Ω
Grid AC line to neutral peak voltage $V_{as}$	30V
Grid AC frequency	60Hz

#### REFERENCES

- [1]:Fekik, Arezki, et al. "Comparative study of two level and three level PWM-rectifier with voltage oriented control." *International Conference on Advanced Intelligent Systems and Informatics*. Springer, Cham, 2018.
- [2]: Yaramasu, V., & Wu, B. (2011, September). Three-level boost converter based medium voltage megawatt PMSG wind energy conversion systems. In *2011 IEEE Energy Conversion Congress and Exposition* (pp. 561-567). IEEE.
- [3]: Qiu, Z., Zhou, K., & Li, Y. (2011, July). Modeling and control of diode rectifier fed PMSG based wind turbine. In *2011 4th international conference on electric utility deregulation and restructuring and power technologies (DRPT)* (pp. 1384-1388). IEEE.
- [4]: Seixas, M., Melício, R., & Mendes, V. M. F. (2014). Fifth harmonic and sag impact on PMSG wind turbines with a balancing new strategy for capacitor voltages. *Energy Conversion and Management*, 79, 721-730.
- [5]:Kumar, A. P., Parimi, A. M., & Rao, K. U. (2015, March). Investigation of small PMSG based wind turbine for variable wind speed. In *2015 International Conference on Recent Developments in Control, Automation and Power Engineering (RDCAPE)* (pp. 107-112). IEEE.
- [6]: Belhadji, L., Bacha, S., & Roye, D. (2011, November). Modeling and control of variable-speed micro-hydropower plant based on axial-flow turbine and permanent magnet synchronous generator (MHPP-PMSG). In *IECON 2011-37th Annual Conference of the IEEE Industrial Electronics Society* (pp. 896-901). IEEE.
- [7]:Sayeef, S., Mendis, N., Muttaqi, K., & Perera, S. (2010, December). Enhanced reactive power support of a PMSG based wind turbine for a remote area power system. In *2010 20th Australasian Universities Power Engineering Conference* (pp. 1-5). IEEE.
- [8]: Ahmed, K. Y., Yahaya, N. Z., Ramani, K., & Asirvadam, V. S. (2017). Modeling and Execution the Control Strategy for the Three-Level Rectifier Based on Voltage Oriented Control. *International Journal of Power Electronics and Drive Systems*, 8(4), 1603.
- [9]: YÜKSEK, H. İ., & ARİFOĞLU, U. (2020). MODELING OF THREE-PHASE THREE-LEVEL RECTIFIER WITH SPACE VECTOR PULSE WIDTH MODULATION METHOD IN MATLAB/SIMULINK PROGRAM. *Sigma: Journal of Engineering & Natural Sciences/Mühendislik ve Fen Bilimleri Dergisi*, 38(1).
- [10]: Park, H. G., Lee, D. C., & Kim, H. G. (2008). Cost-effective converters for micro wind turbine systems using pmsg. *Journal of Power Electronics*, 8(2), 156-162.
- [11]:Liu, Y. (2011). Application of an Intelligent Tuning Algorithm for Three-Level NPC Rectifier for Shipboard Power Distribution.